

Theoretical Study of the Structure and Bonding of a Metal–DNA Base Complex: Al–Guanine

Anastassiia Moussatova, Marco-Vinicio Vázquez, and Ana Martínez*

Instituto de Investigaciones en Materiales, UNAM, Circuito Exterior s/n, Ciudad Universitaria, 04510, Coyoacán, México D.F., México

O. Dolgounitcheva, V. G. Zakrzewski, and J. V. Ortiz

Department of Chemistry, Kansas State University, Manhattan, Kansas 66506-3701

David B. Pedersen and Benoit Simard

Steele Institute for Molecular Sciences, National Research Council of Canada, Ottawa, Ontario K1A 0R6, Canada

Received: May 23, 2003; In Final Form: August 4, 2003

Tautomerism in the most-stable isomers of Al–guanine complexes and their cations is studied with density functional theory and second-order perturbation theory calculations. Electron propagator calculations on vertical ionization energies and Dyson orbitals provide information on the electronic structure in the most-stable neutral doublets, as well as in the corresponding singlets and triplets. The Al–guanine complex consists of a positively charged Al ion with two localized valence electrons coordinated to a negatively charged guanine with an unpaired, delocalized π electron. Three isomers have very similar energies; however, the most-stable form has a markedly different ionization energy. Ionization energies for the second and third forms almost coincide. Predicted ionization energies are in close agreement with recent spectra. In all three cases, the first ionization energy corresponds to a cationic, singlet final state where the unpaired, delocalized π electron on guanine has been removed, whereas the second ionization energy corresponds to the removal of an electron from a 3s-like orbital on the Al ion. Changes in Mulliken charges and optimized structures between neutrals and cations confirm these qualitative conclusions.

Introduction

The potential of some metals to interrupt DNA replication processes has been related to the ability of metals to stabilize tautomers of the DNA bases that are incompatible with the formation of Watson–Crick¹ base pairs and double helices.^{2–4} Studies of metal–DNA base complexes provide valuable thermodynamic and structural information relevant to discussions of metal effects on biological processes involving DNA. The current interest in DNA is not restricted to its role in biology. In particular, the advent of molecular electronics has stimulated interest in regard to the possibility of exploiting this molecule in functional electronic devices and in molecular computing.^{5,6} Metals complexed with DNA may function as electron acceptors or donors and have been successfully used to study charge transport through strands of DNA. This may make DNA useful as a molecular wire in molecular-scale electronic devices. Model complexes have been prepared to explore systematically how different structural and electronic factors may influence electron-transfer reactions. The DNA helix represents a novel medium for examining electron-transfer processes^{5,6} such as charge transport through π -stacks.

In theoretical studies of metal complexes with DNA,^{3,7,8} the best metal-binding site of the DNA bases seems to be N7 (see Figure 1). Most theoretical studies of metal–DNA interactions

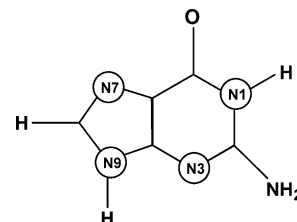


Figure 1. Numbering scheme of guanine.

have focused on guanine complexes in which metal cations are bound to N7.^{7,8} The binding of Na and K cations to guanine is favored at the N7 position, according to recent density functional theory (DFT) calculations.⁹ Little is known about the energetics or properties of isomers of metal–guanine complexes in which the metal binds to sites other than N7. It is not clear whether an analogous affinity for N7 also applies to neutral metal atoms.

A study of gas-phase Al–guanine complexes prepared with laser ablation and characterized by photoionization spectroscopy and mass spectrometry has recently been reported.¹⁰ Photoionization efficiency spectra were collected and used to determine the ionization energies of gas-phase Al–guanine. Variations in the conditions of the laser-ablation source produced two different isomers. In this experiment, the onset of an ion signal can be associated with the adiabatic ionization energies of each complex, whose values are 5.6 ± 0.1 and 4.65 ± 0.01 eV. This interpretation was confirmed by DFT calculations, which suggested that the more stable form, with the larger adiabatic

* Author to whom correspondence should be addressed. E-mail: martina@matilda.iimatercu.unam.mx.

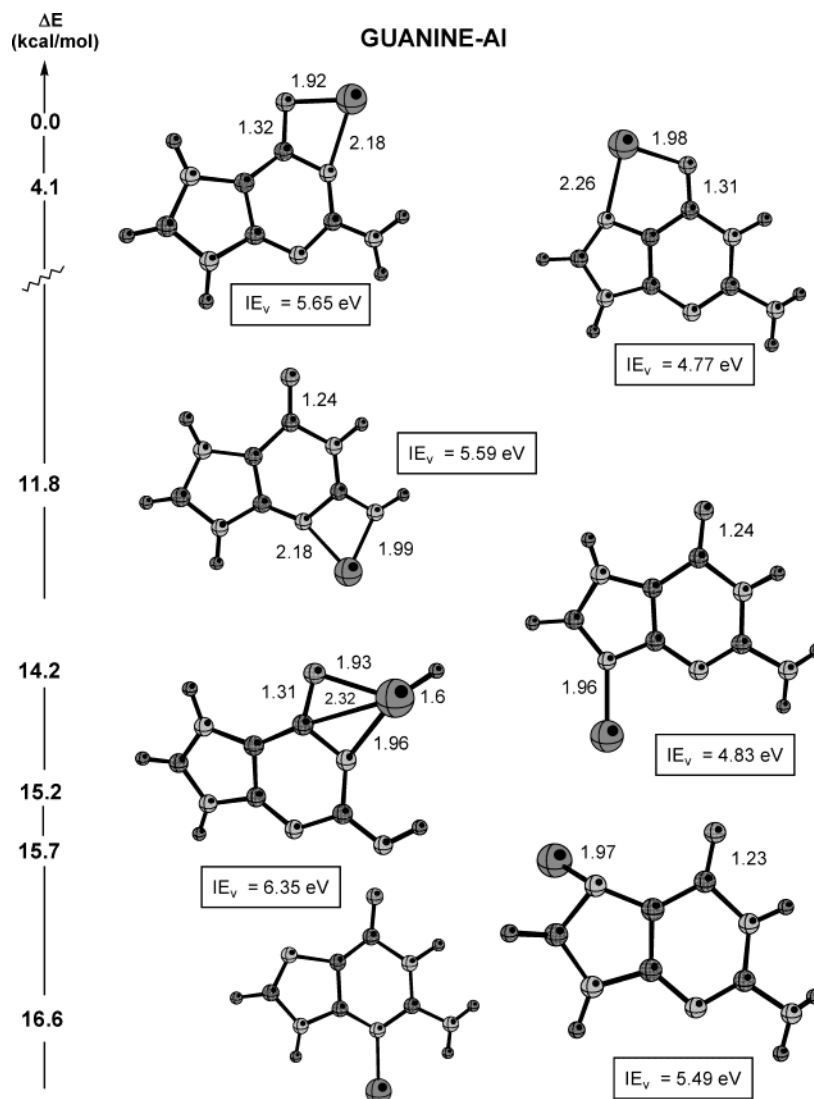


Figure 2. Optimized Al-guanine complexes, relative energies, and vertical ionization energies.

ionization energy, corresponds to a previously unencountered structure where both N atoms in the five-membered ring of guanine are covalently bound to H atoms.

A more thorough theoretical investigation is presented in this work. First, previously ignored tautomeric structures are investigated. Energetic and structural differences between the most-stable forms are examined with second-order perturbation theory, which is a technique more likely to properly describe dispersive interactions between metal centers and guanine. Vertical ionization energies of the most-stable isomers pertaining to cationic singlets and triplets are calculated with *ab initio* electron propagator calculations. Corresponding Dyson orbitals describe differences in the electronic structure between neutral doublets and cationic final states. Assignments of experimental ionization energies are made and qualitative conclusions on the nature of bonding between the Al atom and guanine are drawn from these calculated data. Atomic charges provide qualitative confirmation of these conclusions. In addition, harmonic vibrational frequencies, which are byproducts of the structural investigations, also are presented.

Methods

Density Functional Calculations. All calculations have been performed with Gaussian 98.¹¹ Full geometry optimization without symmetry constraints was performed using the Becke-

Perdew 86 functional¹² and the 6-311+G(2d,p) basis.¹³ A systematic examination of tautomers and metal-guanine coordination geometries was undertaken. Optimized minima were verified with frequency calculations. Visualization of the results was done with the Cerius package¹⁴ and the MOLEKEL¹⁵ program.

Electron Propagator Calculations. The most-stable structures were reoptimized at the MP2/6-311G** level. Electron propagator calculations¹⁶ were performed in the P3 approximation^{17,18} on the reoptimized structures with the same basis, using a modified version of Gaussian 98.¹¹ P3/6-311G** calculations have enjoyed extensive success in the accurate prediction of photoelectron spectra of DNA bases.¹⁹ Dyson orbitals pertaining to each of the ionization energies are plotted with MOLDEN.²⁰ For each ionization energy, there is a Dyson orbital, defined by

$$\varphi^{\text{Dyson}}(x_1) = N^{1/2} \int \Psi_N(x_1, x_2, x_3, \dots, x_N) \times \Psi_{N-1}^*(x_2, x_3, x_4, \dots, x_N) dx_2 dx_3 dx_4 \dots dx_N$$

where the initial and final many-electron states have N and $N - 1$ electrons, respectively. Thus, the Dyson orbital represents an overlap between two states with different numbers of electrons and is a correlated generalization of a canonical, Hartree-Fock orbital.

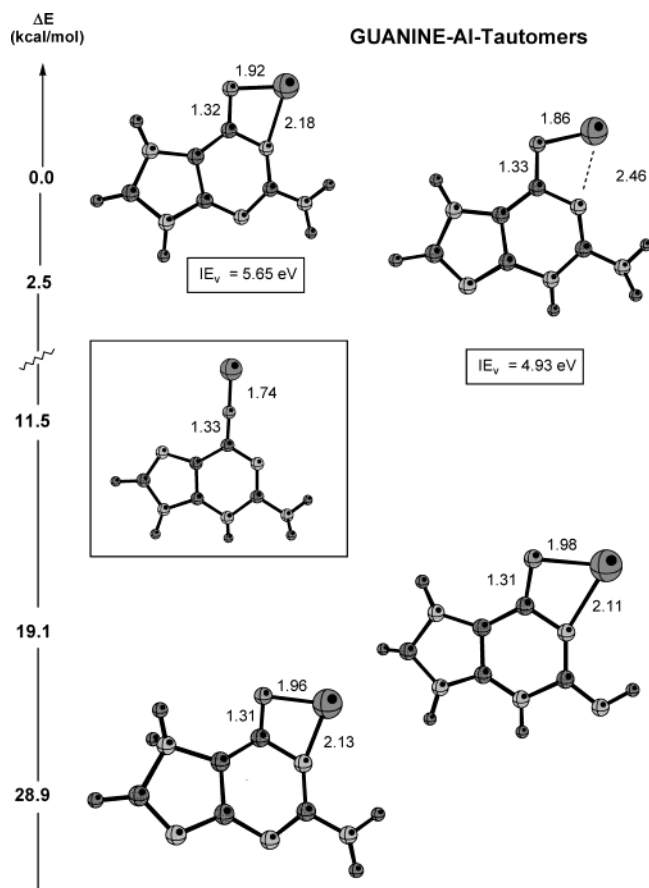


Figure 3. Tautomers of the most-stable Al–guanine complexes, relative energies, and vertical ionization energies.

Results and Discussion

Density Functional Calculations. To determine the position of the Al atom in the Al–guanine complex, several initial geometries were used. We considered the Al atom bound to the N7 or N3 atom, the Al atom inserted into the N1–H bond, and the Al atom bridging the N3 and N9 positions. Figure 2 shows all the geometries that were optimized. Several initial structures where the Al atom interacts with π rings also were examined. Vertical ionization energies are included. There are seven stable structures, with an energy difference of <20 kcal/mol. The most-stable structures are planar, with the Al atom bound to the O atom of the guanine. The first structure has an Al bridge between the N1 and O positions, whereas the second structure has the Al bound to the O and N7 atoms. The energy difference between these two structures is 4.1 kcal/mol. In both isomers, the formation of Al–O–N bridges suggests that this geometry is characteristic of neutral metal–DNA complexes. Similar results have been obtained for Al complexes with cytosine.²¹ The predicted vertical ionization energy of the most stable structure is 5.65 eV. This value is in reasonable agreement with the experimentally determined photoionization threshold of 5.6 ± 0.1 eV. The second experimental value (4.65 ± 0.01 eV) is comparable to the 4.77 eV vertical ionization energy predicted for the second-most-stable isomer of Al–guanine. The binding of metal ions to DNA bases is known to affect the relative stabilities of keto and enol isomers.^{3,22} Complexation with Al stabilizes the keto form of guanine, relative to the enol form.

Several tautomers of each of the two most-stable complexes were optimized. The lowest-energy tautomers of both isomers are shown in Figures 3 and 4, and they are keto forms. In Figure

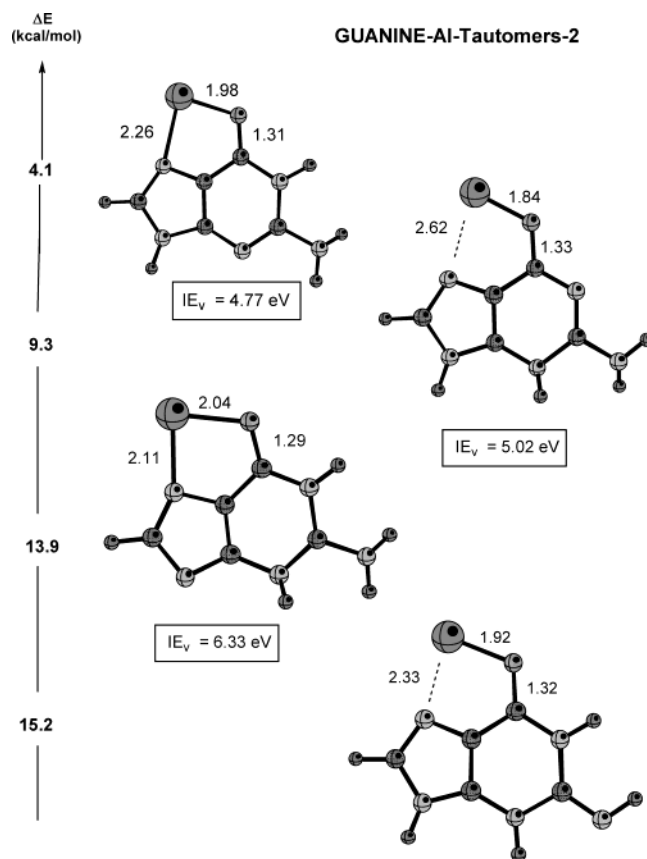


Figure 4. Tautomers of the second Al–guanine complex, relative energies, and vertical ionization energies.

3, the tautomers of the most stable complex are shown. There are two stable structures, with an energy difference of 2.5 kcal/mol. Figure 4 contains the tautomers of the second isomer. The energy differences, with respect to the global minimum, are shown. For this isomer, there are also two stable tautomers; however, the energy difference is slightly higher (5.2 kcal/mol), in comparison with the first isomer (2.5 kcal/mol). For Al–guanine, there are two stable isomers, each with two stable tautomeric forms, within 10 kcal/mol, as can be observed in Figure 5.

These results suggest that the Al atom is bound to the O and N atoms in the Al–guanine species present in the experiment and that Al–guanine bonding chiefly involves aluminum interaction with lone pairs. The most stable isomer is one in which both of the N atoms in the five-membered ring of guanine are bound to H atoms. This unusual form was first proposed in the original experimental report.¹⁰

The lowest species in Figure 5 are the most thermodynamically stable forms of Al–guanine in the gas phase. Chemical properties of both isomers can be expected to differ significantly. A higher ionization energy will characterize a species with a higher oxidation potential. Differences between vertical and adiabatic ionization energies were obtained by optimization of the cations of the most-stable isomers and tautomers. Figure 6 shows the optimized structures of the cationic systems. All systems are singlets, whereas the neutrals are doublets. Significant structural changes occur between the neutral (Figure 5) and cationic (Figure 6) geometries. The biggest difference pertains to the Al–N bond distance. For the cationic species, this bond length is larger than that for the neutral geometry. The stability order of the cationic systems is different. The most stable cation corresponds to the third neutral structure. The most

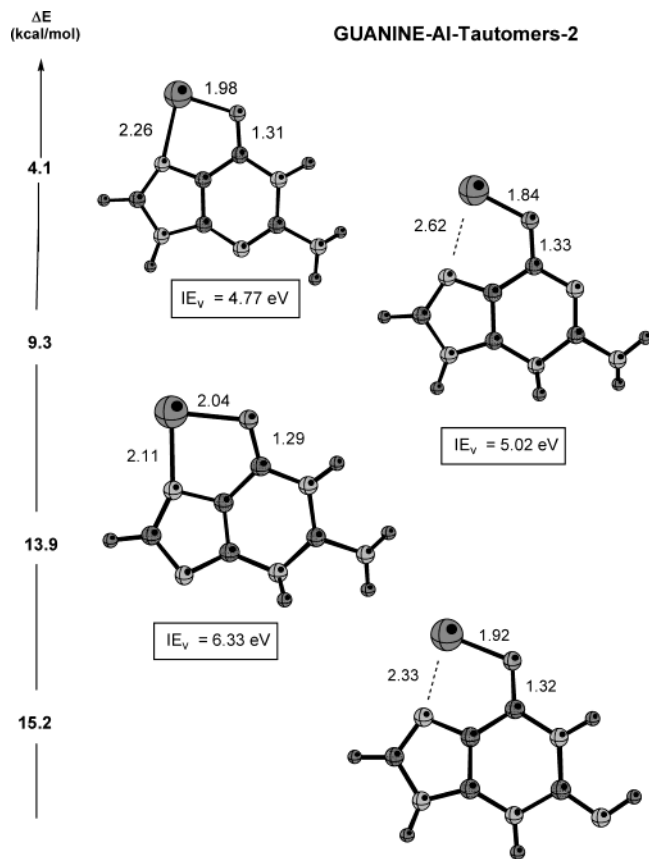


Figure 5. Four most-stable Al-guanine complexes, relative energies, and vertical ionization energies.

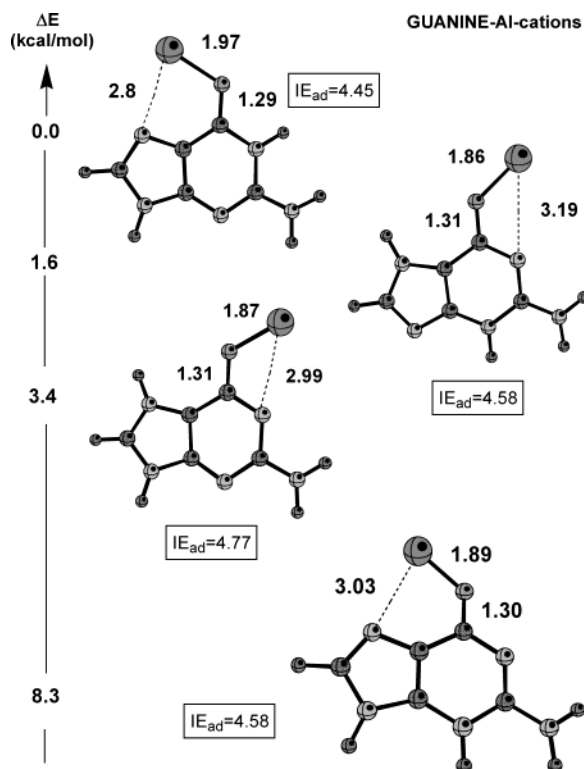


Figure 6. Optimized cationic structures corresponding to the four most-stable neutral structures, relative energies, and adiabatic ionization energies.

stable neutral structure corresponds to the third one of the cation. This reordering might be expected when the energy differences are so small. In contrast, vertical and adiabatic ionization

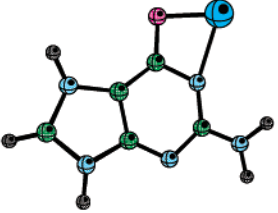
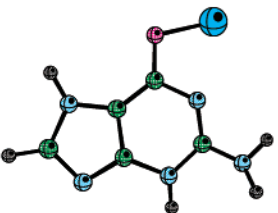
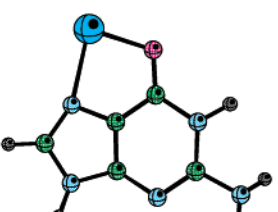
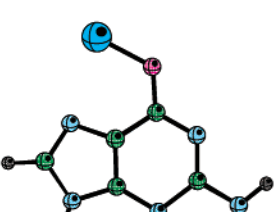
energies differ markedly, because of the distinct geometries of neutrals and cations.

Harmonic vibrational frequencies and Mulliken atomic charges are shown in Table 1. The charges provide an approximate guide to differences in electronic distributions pertaining to vertical and adiabatic ionization energies of the neutral complexes. (Charges for cations are given for the optimized neutral and cationic geometries.) These charges indicate that the O atom is negative and the Al atom is positive in all the isomers (neutral and cationic), as expected from the electronegativities of oxygen and aluminum. Because the aluminum is positive and the overall charge of the guanine is negative, the complex seems to have ionic character.

Electron Propagator Calculations. Electron propagator calculations were preceded by MP2/6-311G** reoptimizations of the three lowest structures found with DFT methods. Dispersion interactions between Al and guanine are likely to be described better with MP2 than with DFT methods, and significant differences between optimized geometries are obtained. Although the lowest structure undergoes very little rearrangement of the nuclei, in the other two structures, there is somewhat greater nonplanarity in the Al positions and in the pyramidalization of the amine nitrogen. In addition, the order of the second and third isomers of Figure 5 is reversed and the corresponding MP2 isomerization energies, relative to the lowest structure, are 7.9 and 11.2 kcal/mol. However, spin contamination is not uniform in the three structures. The $\langle S^2 \rangle$ values are 0.77, 0.86, and 0.92 for the three structures, respectively. Therefore, spin-projected MP2 energies were evaluated. Projected values of $\langle S^2 \rangle$ are 0.75, 0.76, and 0.77, respectively. Corresponding relative energies for the second and third isomers are 4.2 and 5.5 kcal/mol. Relative energies at the MP2 level, especially of this low magnitude, are not definitive; however, they do indicate the need to consider all low-lying isomers in the interpretation of experiments based on laser-ablation synthesis of the gas-phase species.

Results of P3/6-311G** electron propagator calculations on the vertical ionization energies of the three lowest isomers are shown in Table 2. In each case, the lowest singlet and triplet states of the cation were studied. For the lowest isomer, the lowest vertical ionization energy is 5.99 eV. This value is somewhat higher than the DFT value and the experimental value of 5.6 ± 0.1 eV that pertains to the photoionization threshold. The latter datum is likely to apply to an adiabatic ionization energy, and the calculated result provides a reasonable upper bound. In Figure 7, the Dyson orbital pertaining to the first ionization energy is shown. The largest amplitudes in this π orbital are found on the two C atoms between the N1 and N7 positions. Contributions from atoms in the five-member ring are also important. Minor lobes on the O and N1 centers also are present. Thus, the least-bound electron is localized on the guanine; Al contributions are very small. One may infer that the neutral complex may be described approximately as a complex of a guanine anion and an Al cation. The importance of such charge-transfer states in metal-DNA complexes was proposed in a previous publication regarding the photochemistry of cytosine.²¹ When an electron is removed from this Dyson orbital, the Al cation is subject to an enhanced positive charge at the nearest C atom and it rotates to a relatively remote position while preserving its strong ionic bond with oxygen. A vertical ionization energy corresponding to an excited state of the cation of the lowest structure is predicted at 7.42 eV. Here, the final state is a triplet. In the Dyson orbital plot, the largest amplitudes are localized in an s-like lobe on the aluminum.

TABLE 1: Harmonic Vibrational Frequencies and Mulliken Atomic Charges for the Most-Stable Neutral Complexes^a

	Atomic charges (neutral)	Atomic charges (cations)	Harmonic Frequencies
	Al = 0.24 O = -0.55 C = 0.37 N = -0.43	not optimized Al = 0.39 O = -0.48 C = 0.46 N = -0.39	63 129 134 179 219 273 308 332 383 405 418 440 462 481 495 569 615 620 668 692 699 739 799 874 1014
		optimized Al = 0.56 O = -0.58 C = 0.49 N = -0.45	1041 1048 1078 1145 1195 1284 1296 1326 1368 1397 1417 1458 1568 1582 1607 3052 3495 3560 3613
	Al = 0.23 O = -0.57 C = 0.42 N = -0.42	not optimized Al = 0.45 O = -0.49 C = 0.46 N = -0.38	37 63 110 188 203 253 300 320 329 367 375 451 462 492 564 566 598 607 615 670 683 692 815 908 996
		optimized Al = 0.60 O = -0.59 C = 0.52 N = -0.48	1019 1044 1111 1150 1196 1244 1268 1334 1366 1425 1459 1468 1543 1564 1606 3195 3437 3481 3546 3568
	Al = 0.12 O = -0.53 C = 0.45 N = -0.32	not optimized Al = 0.40 O = -0.44 C = 0.50 N = -0.28	55 105 151 156 205 275 292 322 337 368 393 398 456 475 512 524 580 593 604 658 688 706 809 895 972
		optimized Al = 0.52 O = -0.51 C = 0.56 N = -0.31	993 1069 1101 1131 1230 1248 1305 1334 1348 1414 1435 1510 1543 1585 1594 3214 3455 3493 3537 3558
	Al = 0.25 O = -0.58 C = 0.52 N = -0.30	not optimized Al = 0.46 O = -0.50 C = 0.58 N = -0.26	58 76 109 170 238 276 289 321 352 405 436 452 472 540 543 588 607 640 648 683 707 745 824 892 917
		optimized Al = 0.55 O = -0.55 C = 0.57 N = -0.31	1039 1069 1118 1150 1223 1251 1306 1313 1344 1386 1404 1484 1510 1576 1601 3192 3281 3382 3515 3539

^a “Optimized” denotes the atomic charge in the cation for a cationic geometry, and “not optimized” represents that for an optimized neutral geometry.

In the second-most-stable structure, ionization energies pertaining to singlet and triplet final states are calculated to be 4.52 and 6.82 eV, respectively. The former datum is in good agreement with the experimental value of 4.65 ± 0.01 eV. The presence of an isomer with a lower ionization threshold is produced by the introduction of ammonia gas in the plasma source. Dyson orbitals for this structure (Figure 8) are approximately similar to their counterparts in the

lowest structure. For the lowest ionization energy, where the final state is a singlet, the Dyson orbital still has large amplitudes on the C atom that is nearest to the Al atom. As in the first structure, the removal of an electron from this orbital causes the Al cation to rotate away from the six-member ring while maintaining its strong bond to oxygen. Some distortion of the Dyson orbital, with respect to its counterpart in the lowest isomer, is obtained. In the second

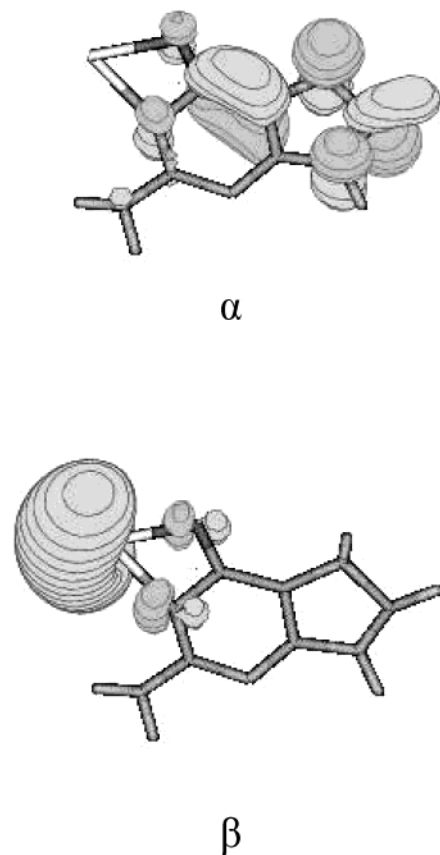


Figure 7. Dyson orbitals for ionization energies pertaining to singlet (α) and triplet (β) states of the cation of the lowest structure.

TABLE 2: P3/6-311G Vertical Ionization Energies**

final state	vertical ionization energy (eV)		
	structure 1	structure 2	structure 3
singlet	5.99	4.52	5.82
triplet	7.42	6.82	7.23

Dyson orbital, localization on an s-like lobe of the aluminum is observed again.

Deviations from planarity in the third structure are evident from an examination of the corresponding Dyson orbitals in Figure 9. For the singlet final state, the vertical ionization energy is 5.82; for the triplet final state, the corresponding transition energy is 7.23 eV. The near coincidence of the lowest vertical ionization energy calculated for this isomer with its counterpart for the lowest isomer (5.99 eV) and the small isomerization energy that separates the two neutral species suggests that the experimental peak could have contributions from both isomers. In the first Dyson orbital, there is some mixing between σ and π lobes. The distribution of this orbital over the atomic centers also is changed, relative to the two lower isomers. As mentioned previously, there is little localization on aluminum in this case. The opposite is true for the second Dyson orbital, which is dominated by an s-like lobe on aluminum.

For all three structures, the least-bound electron corresponds to a delocalized Dyson orbital that is spread over many guanine atoms. In the two lowest structures, the Dyson orbital is clearly of the π type. At higher ionization energies, there are corresponding Dyson orbitals, which consist chiefly of s-functions on aluminum. Therefore, the neutral complex consists approximately of a guanine anion and an Al cation with two valence electrons in an s-like lobe. A bound guanine anion with an unpaired π electron has not yet been encountered in the gas phase.

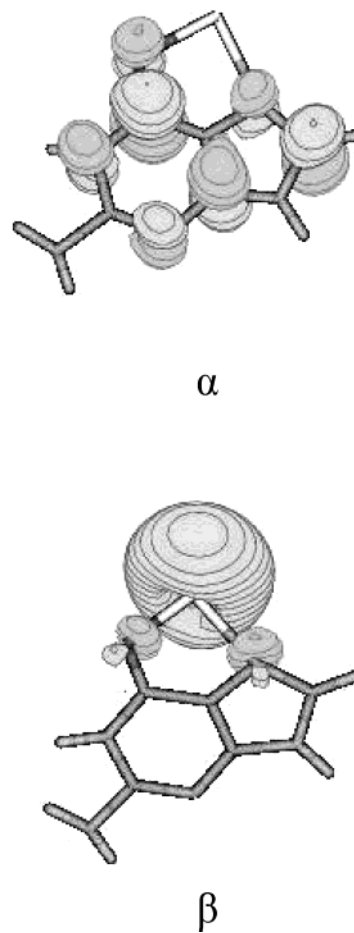


Figure 8. Dyson orbitals for ionization energies pertaining to singlet (α) and triplet (β) states of the cation of the second-lowest structure.

Conclusions

The most stable structure of the Al–guanine complex has two N–H bonds on the five-member ring. The metal atom bridges between the O and N1 positions. This unprecedented structure has an ionization energy that may be assigned to the photoionization threshold at 5.6 ± 0.1 eV, which has been observed in recent experiments.¹⁰ An electron is removed from a π Dyson orbital that resides chiefly on the guanine. In the corresponding cationic state, the oxygen-bound Al atom is more remote from the N1 atom. Depletion of the electronic charge in the nearest C atom, which has large amplitudes in the Dyson orbital, explains this structural change in the cation. A higher ionization energy is predicted to correspond to a Dyson orbital that consists chiefly of s-functions on aluminum.

At an energy ~ 4 kcal/mol higher, one can find an Al–guanine complex where the metal atom bridges between the O and N7 atoms. The ionization energy of this species is similar to that of the spectral feature at 4.65 ± 0.01 eV, which is produced under different source conditions.¹⁰ The Dyson orbitals corresponding to the first and second ionization energies calculated with electron propagator theory remain localized on guanine and on the metal atom, respectively. Structural changes in the cations are responses to the removal of negative charge from the C atom nearest to the Al atom.

A tautomer of the lowest structure is the third-most-stable isomer in MP2 calculations, but it is within 1 kcal/mol of the second structure. Ionization energies of this structure are similar to those of the lowest isomer. The distribution of the Dyson orbitals also is qualitatively similar. The observed spectral

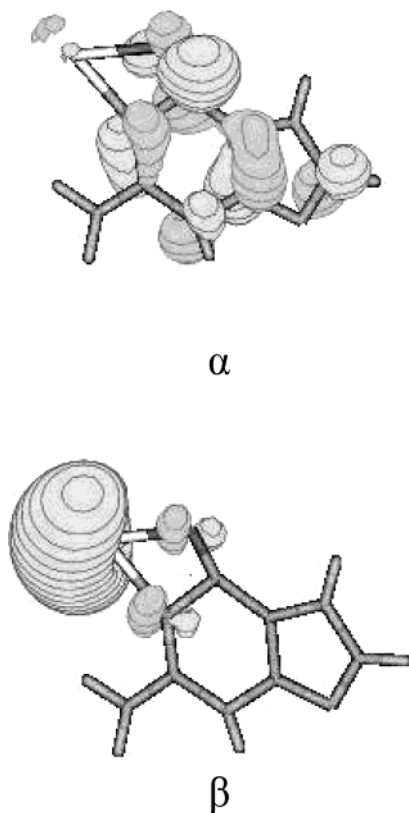


Figure 9. Dyson orbitals for ionization energies pertaining to singlet (α) and triplet (β) states of the cation of the third-lowest structure.

feature at 5.6 ± 0.1 eV also may have contributions from this structure. Many less-stable tautomeric forms also have been examined.

The Al–guanine complex exhibits considerable charge transfer from Al to guanine in all of its low-lying tautomers. The first two ionization energies in each structure correspond to the removal of electrons from a singly occupied, delocalized π orbital on guanine to produce a closed-shell cation or from a doubly occupied, localized, 3s-like orbital on Al to produce a triplet cation.

Acknowledgment. This work was supported by the National Science Foundation (under Grant No. CHE-0135823), DGAPA (No. IN124602), and CONACYT-NSF (No. E120.1778/2001). The authors acknowledge Sara Jiménez Cortés and María Teresa Vázquez for technical support and DGSCA/UNAM (México) for providing computer time.

References and Notes

- (1) Watson, J. D.; Crick, F. H. C. *Nature* **1953**, *171*, 737.
- (2) Pichjerra, F.; Hotheinrich, D.; Zangrando, E.; Lipperte, B.; Ranacciao, L. J. *Bio. Inorg. Chem.* **1996**, *1*, 319.
- (3) Spöner, J.; Spöner, J. E.; Gorb, L.; Leszczynski, J.; Lippert, B. *J. Phys. Chem. A* **1999**, *103*, 11406.
- (4) Müller, J.; Sigel, R. K. O.; Lippert, B. *J. Inorg. Biochem.* **2000**, *79*, 261.
- (5) Berlin, Y. A.; Burin, A. L.; Ratner, M. A. *Superlattices Microstruct.* **2000**, *28*, 241.
- (6) Murphy, C. J.; Arkin, M. R.; Jenkins, Y.; Ghatlia, N. D.; Bossmann, S. H.; Turro, N. J.; Barton, J. K. *Science* **1993**, *262*, 1025.
- (7) Spöner, J.; Sabat, M.; Gorb, L.; Leszczynski, J.; Lippert, B.; Hobza, P. *J. Phys. Chem. B* **2000**, *104*, 7535.
- (8) Burda, J. V.; Spöner, J.; Leszczynski, J. *J. Biol. Inorg. Chem.* **2000**, *5*, 178.
- (9) Russo, N.; Toscano, M.; Grand, A. *J. Am. Chem. Soc.* **2001**, *123*, 10272.
- (10) Pedersen, D. B.; Simard, B.; Martinez, A.; Moussatova, A. *J. Phys. Chem. A* **2003**, *107*, 6464.
- (11) Frisch, M. J.; Trucks, G. W.; Schlegel, H. B.; Scuseria, G. E.; Robb, M. A.; Cheeseman, J. R.; Zakrzewski, V. G.; Montgomery, J. A., Jr.; Stratmann, R. E.; Burant, J. C.; Dapprich, S.; Millam, J. M.; Daniels, A. D.; Kudin, K. N.; Strain, M. C.; Farkas, O.; Tomasi, J.; Barone, V.; Cossi, M.; Cammi, R.; Mennucci, B.; Pomelli, C.; Adamo, C.; Clifford, S.; Ochterski, J.; Petersson, G. A.; Ayala, P. Y.; Cui, Q.; Morokuma, K.; Malick, D. K.; Rabuck, A. D.; Raghavachari, K.; Foresman, J. B.; Cioslowski, J.; Ortiz, J. V.; Stefanov, B. B.; Liu, G.; Liashenko, A.; Piskorz, P.; Komaromi, I.; Gomperts, R.; Martin, R. L.; Fox, D. J.; Keith, T.; Al-Laham, M. A.; Peng, C. Y.; Nanayakkara, A.; Gonzalez, C.; Challacombe, M.; Gill, P. M. W.; Johnson, B. G.; Chen, W.; Wong, M. W.; Andres, J. L.; Head-Gordon, M.; Replogle, E. S.; Pople, J. A. *Gaussian 98*, revision A.8; Gaussian, Inc.: Pittsburgh, PA, 1998.
- (12) (a) Becke, A. D. *Phys. Rev. A* **1988**, *38*, 3098. (b) Perdew, J. P. *Phys. Rev. B* **1986**, *33*, 8822–8824.
- (13) (a) Krishnan, R.; Binkley, J. S.; Seeger, R.; Pople, J. A. *J. Chem. Phys.* **1980**, *72*, 650. (b) Clark, T.; Chandrasekhar, J.; Spitznagel, G. W.; Schleyer, P. v. R. *J. Comput. Chem.* **1983**, *4*, 294. (c) Frisch, M. J.; Pople, J. A.; Binkley, J. S. *J. Chem. Phys.* **1984**, *80*, 3265. (d) McLean, A. D.; Chandler, G. S. *J. Chem. Phys.* **1980**, *72*, 5639.
- (14) *Cerius2*, Force Field-Based Simulations, April 1997; Molecular Simulations, Inc.: San Diego, CA, 1997.
- (15) Flükiger, P.; Lüthi, H. P.; Portmann, S.; Weber, J. *MOLEKEL 4.2*; Swiss Center for Scientific Computing: Manno, Switzerland, 2000–2002.
- (16) Ortiz, J. V. *Adv. Quantum Chem.* **1999**, *35*, 33.
- (17) Ortiz, J. V. *J. Chem. Phys.* **1996**, *104*, 7599.
- (18) Ferreira, A. M.; Seabra, G.; Dolgounitcheva, O.; Zakrzewski, V. G.; Ortiz, J. V. In *Quantum-Mechanical Prediction of Thermochemical Data*; Cioslowski, J., Ed.; Kluwer: Dordrecht, The Netherlands, 2001; Vol. 131.
- (19) (a) Dolgounitcheva, O.; Zakrzewski, V. G.; Ortiz, J. V. *J. Phys. Chem. A* **2003**, *107*, 822. (b) Dolgounitcheva, O.; Zakrzewski, V. G.; Ortiz, J. V. *Int. J. Quantum Chem.* **2002**, *90*, 1547. (c) Dolgounitcheva, O.; Zakrzewski, V. G.; Ortiz, J. V. *J. Phys. Chem. A* **2002**, *106*, 8411. (d) Dolgounitcheva, O.; Zakrzewski, V. G.; Ortiz, J. V. *J. Phys. Chem. A* **2001**, *105*, 8782. (e) Dolgounitcheva, O.; Zakrzewski, V. G.; Ortiz, J. V. *J. Am. Chem. Soc.* **2000**, *122*, 12304. (f) Dolgounitcheva, O.; Zakrzewski, V. G.; Ortiz, J. V. *Int. J. Quantum Chem.* **2000**, *80*, 831.
- (20) Schaftenaar, G. *MOLDEN 3.4*; CAOS/CAMM Center: Nijmegen, The Netherlands, 1998.
- (21) Pedersen, D. B.; Zgierski, M. Z.; Denomme, S.; Simard, B. *J. Am. Chem. Soc.* **2002**, *124*, 6686.
- (22) Müller, J.; Sigel, R. K. O.; Lippert, B. *J. Inorg. Biochem.* **2000**, *79*, 261.